Radiative and Dynamical Feedbacks over the Equatorial Cold Tongue: Results from Nine Atmospheric GCMs

D.-Z. Sun and T. Zhang

CIRES/Climate Diagnostics Center, and NOAA/Earth System Research Laboratory, Boulder, Colorado

C. Covey and S. A. Klein

Lawrence Livermore National Laboratory, Livermore, California

W. D. Collins, J. J. Hack, J. T. Kiehl, and G. A. Meehl

National Center for Atmospheric Research, Boulder, Colorado

I. M. Held

NOAA/Geophysical Fluid Dynamics Laboratory, Princeton, New Jersey

M. Suarez

National Aeronautics and Space Administration, Greenbelt, Maryland

ABSTRACT

The equatorial Pacific is a region with strong negative feedbacks. Yet coupled general circulation models (GCMs) have exhibited a propensity to develop a significant SST bias in that region, suggesting an unrealistic sensitivity in the coupled models to small energy flux errors that inevitably occur in the individual model components. Could this "hypersensitivity" exhibited in a coupled model be due to an underestimate of the strength of the negative feedbacks in this region? With this suspicion, the feedbacks in the equatorial Pacific in nine atmospheric GCMs (AGCMs) have been quantified using the interannual variations in that region and compared with the corresponding calculations from the observations. The nine AGCMs are the NCAR Community Climate Model version 1 (CAM1), the NCAR Community Climate Model version 2 (CAM2), the NCAR Community Climate Model version 3 (CAM3), the NCAR CAM3 at T85 resolution, the NASA Seasonal-to-Interannual Prediction Project (NSIPP) Atmospheric Model, the Hadley Centre Atmospheric Model (HadAM3), the Institut Pierre Simon Laplace (IPSL) model (LMDZ4), the Geophysical Fluid Dynamics Laboratory (GFDL) AM2p10, and the GFDL AM2p12. All the corresponding coupled runs of these nine AGCMs have an excessive cold tongue in the equatorial Pacific.

The net atmospheric feedback over the equatorial Pacific in the two GFDL models is found to be comparable to the observed value. All other models are found to have a weaker negative net feedback from the atmosphere—a weaker regulating effect on the underlying SST than the real atmosphere. Except for the French (IPSL) model, a weaker negative feedback from the cloud albedo and a weaker negative feedback from the atmospheric transport are the two leading contributors to the weaker regulating effect from the atmosphere. The underestimate of the strength of the negative feedbacks by the models is apparently linked to an underestimate of the equatorial precipitation response. All models have a stronger water vapor feedback than that indicated in Earth Radiation Budget Experiment (ERBE) observations. These results confirm the suspicion that an underestimate of the regulatory effect from the atmosphere over the equatorial Pacific region is a prevalent problem. The results also suggest, however, that a weaker regulatory effect from the atmosphere is unlikely solely responsible for the hypersensitivity in all models. The need to validate the feedbacks from the ocean transport is therefore highlighted.

1. Introduction

The equatorial Pacific is a region with strong negative feedbacks. Ramanathan and Collins (1991) first observed that a SST anomaly in the central Pacific triggers a negative response from the shortwave forcing of clouds—deep clouds reflect more (less) solar radiation back to space in response to a positive (negative) SST changes. They even postulated that this negative feedback of cloud albedo may be a "thermostat" of the Tropics. Subsequent studies point out the importance of the feedbacks from the atmospheric and oceanic dynamics (Fu et al. 1990; Wallace 1992; Pierrehumbert 1995; Sun and Liu 1996). In an attempt to assess the relative importance of the cloud albedo feedback and the feedback from dynamics, Sun and Trenberth (1998) used the best data available and quantified the changes in the heat transport in the atmosphere and in the ocean associated with the 1986–87 El Niño warming in addition to calculating the changes in the radiative fluxes. The results show that the negative feedback from the cloud albedo is actually a smaller player compared to the other two negative feedbacks in the equatorial Pacific region, namely, the feedback from the heat transport by the atmospheric circulation and the feedback from the poleward heat transport by the ocean circulation. The negative feedback from the poleward ocean heat transport is found to be twice as strong as the negative feedback from the atmospheric transport. The latter is, in turn, twice as strong as the cloud albedo feedback. Against this background, the prevalence of a profound bias in the central equatorial Pacific in coupled GCMs is a surprise. We acknowledge that there is no lack of causes of initial cooling to the equatorial SST due to imperfections in the individual components. For example, the lack of phytoplankton in the model ocean could lead to an underestimate of the solar radiation absorbed by the ocean (Murtugudde et al. 2002). The lack of sufficient vertical resolution of the ocean model may also lead to an excessive cooling of the surface ocean (Stockdale et al. 1998). The winds are not perfect in the atmospheric models and the errors may induce excessive equatorial upwelling upon coupling. The surface heating from the atmospheric model may also be too weak, even with the observed SST (Sun et al. 2003). However, the effects of these initial errors in the individual model components on the equilibrium SST of the coupled model depend on the feedbacks (Kiehl 1998; Sun et al. 2003). Given the existence of a myriad of strong negative feedbacks, why does the SST in this region simulated by a coupled model appear to be sensitive to flux errors in the model components? Could it be that the strength of one or more negative feedbacks in the model is underestimated? Or alternatively, could it be that the strength of one or more positive feedbacks in the model is overestimated?

A preliminary attempt to answer these questions was made by Sun et al. (2003). By examining the response of radiative and dynamical fluxes to ENSO in the National Center for Atmospheric Research (NCAR) Community Climate Model version 3 (CCM3), they noted that the negative feedback of cloud albedo is substantially underestimated in the model. In further light of some coupled experiments, they put forward the hypothesis that a weaker regulating effect from the atmosphere may be a significant contributor to the development of an excessive cold tongue in the corresponding coupled model. The purpose of this study is to extend the analysis of Sun et al. (2003) to eight additional models whose corresponding coupled runs also have an excessive cold tongue in the equatorial Pacific. The almost ubiquitous presence of an excessive cold tongue in the equatorial Pacific in the coupled GCMs offers a unique opportunity to understand the causes for this syndrome: a hypothesis developed in one model can be readily tested against other models.

2. Methods

The study employs the same method as in Sun et al. (2003). We use the surface warming and cooling associated with ENSO as the forcing signal. We will then examine how radiative fluxes at the top of the atmosphere (TOA) and the vertically integrated transport of energy in the atmosphere vary in relation to the underlying SST. We quantify the feedbacks by linearly regressing the corresponding fluxes to the SST using their respective interannual variations.

The cloud and water vapor feedbacks in this paper are measured in the same way as that of Cess and Potter (1988): water vapor feedback is equated with the change in the greenhouse effect in the clear sky region, and the cloud feedbacks are equated with the corresponding changes in the longwave and shortwave cloud forcing. These measures are not the same as the measures of Wetherald and Manabe (1988) that used offline radiative transfer calculations to obtain the true partial derivatives (Soden et al. 2004). The measures of Cess and Potter tend to overestimate the feedback from the greenhouse effect of water vapor and underestimate the feedback from the greenhouse effect of clouds. However, provided the feedbacks in the models are measured in the same way as in the observations, the errors revealed in the analysis are still true errors in the models. The available radiation data measure the feedbacks of water vapor and clouds on the ENSO time

scale in the form of used by Cess and Potter (1988). Also, the concern here is more with the combined effect of water vapor and cloud feedbacks on the response in the net surface heat flux into the ocean—the net atmospheric feedback—than with the accuracy in the definition of individual feedbacks of water vapor and clouds; the distinctions between the measures of Cess and Potter (1988) and Wetherald and Manabe (1988) of the individual feedbacks of water vapor and clouds are considered less important.

The observational data for radiation fluxes come from the Earth's Radiation Budget Experiment (ERBE) (Barkstrom et al. 1989). The data for the atmospheric transport is calculated from the National Centers for Environmental Prediction–National Center for Atmospheric Research (NCEP–NCAR) reanalysis by making use of the global observations of temperature, humidity, and winds (Trenberth and Guillemot 1998). The data for the surface heat flux are obtained through the energy balance equation of the atmosphere—the surface heat flux is calculated by combining the net radiation flux from ERBE, the atmospheric transport, and the heat storage in the atmosphere (Trenberth et al. 2001). The data for the surface heat flux are considered the best available. Nonetheless, we will also calculate the feedback from the surface heat flux and the feedback from the atmospheric transport by making use of the 40-yr European Centre for Medium-Range Weather Forecasts (ECMWF) Re-Analysis (ERA-40) (Uppala et al. 2004). (The ERA-40 does not have data for the atmospheric transport. We will calculate it as the difference between the net surface heat flux and the net radiative flux at the top of the atmosphere from ERBE.)

The model data are from the runs of the Atmospheric Model Intercomparison Project (AMIP) over the ERBE period. The AMIP runs have the observed, time-varying SST as the boundary conditions. Therefore, the model atmosphere is subject to the same SST forcing as the real atmosphere.

The models that have been analyzed are the models that have a corresponding coupled run without the use of flux adjustment. These models are 1) the NCAR Community Climate Model version 1 (CAM1) (Kiehl et al. 1998), 2) the NCAR Community Climate Model version 2 (CAM2) (Collins et al. 2003), 3) the NCAR Community Climate Model version 3 (CAM3) at T42, 4) the NCAR CAM3 at T85 (Collins et al. 2004), 5) the NASA Seasonal-to-Interannual Prediction Project (NSIPP) model (Chou and Suarez 1996; Suarez 1995), 6) the Hadley Centre model (Collins et al. 2001), 7) the Institut Pierre Simon Laplace (IPSL) LMDZ4 (Hourdin et al. 2005, manuscript submitted to *Climate Dyn.*),

8) the Geophysical Fluid Dynamics Laboratory (GFDL) AM2p10, and 9) the GFDL AM2p12 (GFDL Global Atmospheric Model Development Team 2004). [The GFDL AM2p10 is an earlier version of the GFDL AM2p12. The main differences between the two versions are in the use of boundary layer schemes and in the vertical layers. The AM2p10 uses the boundary layer scheme of Mellor and Yamada (1974) while the AM2p12 uses the boundary layer scheme of Lock et al. (2000). The AM2p12 has 24 vertical layers while the AM2p10 has 18 vertical layers.]

The nine models involve the use of five different schemes for moist convection. The NCAR models use the deep convection scheme by Zhang and McFarlane (1995) and the shallow convection scheme by Hack (1994). The NASA NSIPP model and the two GFDL models use the relaxed Arakawa–Schubert (RAS) scheme (Moorthi and Suarez 1992). The Hadley Centre model uses a mass-flux scheme (Gregory and Rowntree 1990) based on the bulk cloud model of Yanai et al. (1973). The French IPSL LMDZ4 uses a revised version of the Emanuel (1991) scheme (Grandpeix et al. 2004). The nine models also have different vertical and horizontal resolutions. The vertical resolutions vary from 18 layers (NCAR CAM1) to 34 layers (NASA NSIPP). Except for the NCAR CAM3 at T85, the horizontal resolutions of the models are more comparable, while the horizontal resolutions in the remaining eight models vary from about $3.8° \times 2.5°$ in the Hadley Centre model to $2.5° \times 2.0°$ in the GFDL and the NASA models. Despite the many differences in these atmosphere models, gauged by the meridional and zonal SST gradients over the equatorial Pacific, all their corresponding coupled models have an excessive cold tongue over the central equatorial Pacific (Fig. 1).

3. Results

The estimates of the feedbacks from these models over the central equatorial Pacific region (5°S–5°N, 150°–250°E) are summarized in Table 1. Note that these feedbacks are regional feedbacks on the ENSO time scale. The results presented in the table are not sensitive to small changes in the boundaries chosen for the calculations. The definition of the symbols and the procedure of the calculations are the same as in Sun et al. (2003): $\partial G_a/\partial T$ is the water vapor feedback, $\partial C_l/\partial T$ is the feedback from the longwave forcing of clouds (the greenhouse effect of clouds), $\partial C_s/\partial T$ is the feedback from the shortwave forcing of clouds, and $\partial D_a/\partial T$ is the feedback from the atmospheric transport. Here

$$\frac{\partial F_a}{\partial T} = \frac{\partial G_a}{\partial T} + \frac{\partial C_l}{\partial T} + \frac{\partial C_s}{\partial T} + \frac{\partial D_a}{\partial T}$$
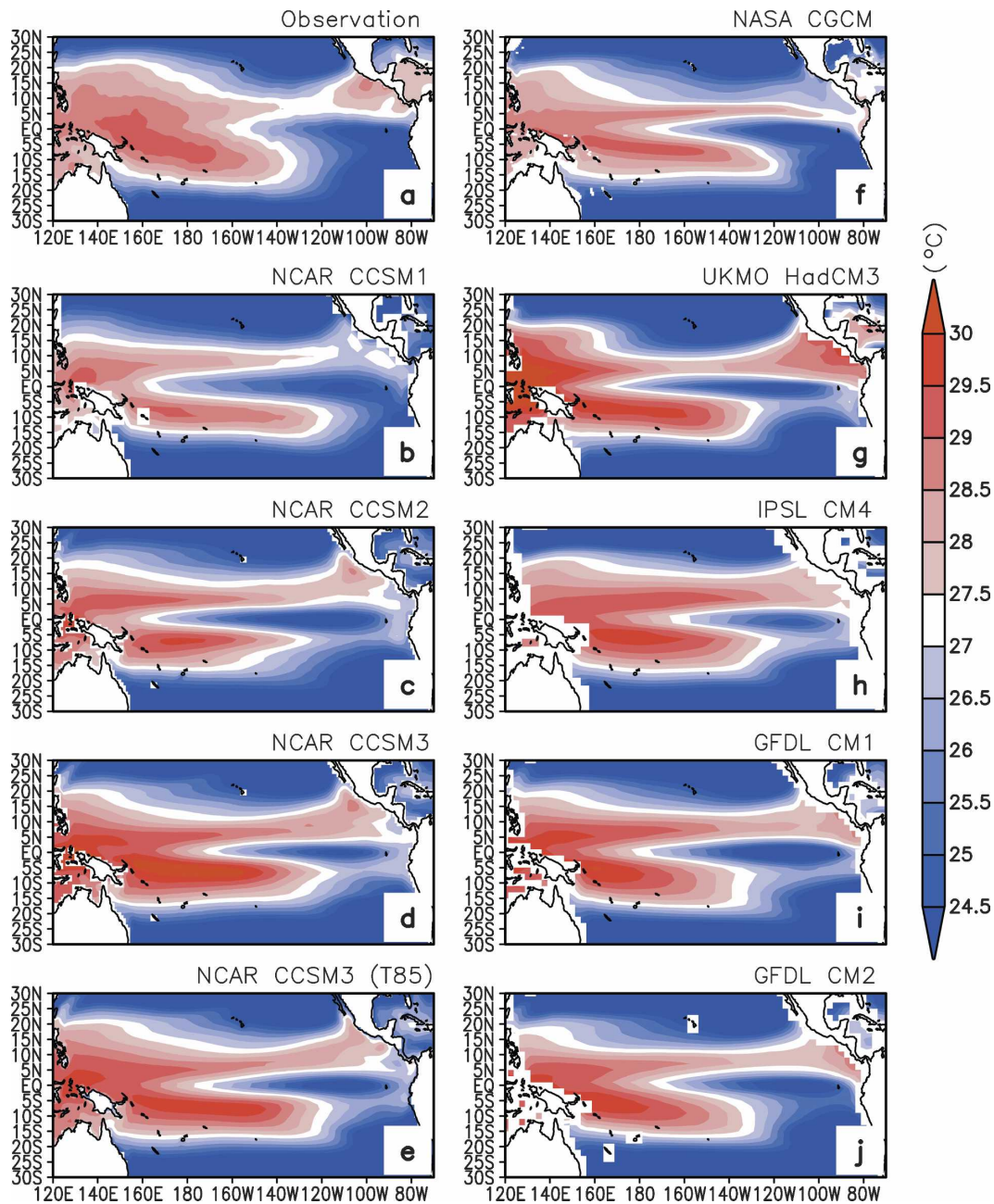
FIG. 1. Climatological annual mean tropical Pacific SST from observations (Rayner et al. 1996) and nine coupled climate models: the NCAR Community Climate System Model version 1 (CCSM1) (Boville and Gent 1998), the NCAR CCSM2 (Kiehl and Gent 2004), the NCAR CCSM3 (http://www.ccsm.ucar.edu/experiments/ccsm3.0/), the NASA CGCM (http://nsipp.gsfc.nasa.gov/data_req/coupled/coupl_data_main.htl), the coupled model of the Hadley Centre (HadCM3; Collins et al. 2001), the French IPSL climate system model (IPSL-CM4; Marti et al. 2005), and the two versions of the coupled models from GFDL (Delworth et al. 2006). The atmospheric components of the nine coupled models are, respectively, the NCAR CAM1, the NCAR CAM2, the NCAR CAM3 at the standard T42 resolution, the NCAR CAM3 at T85 resolution, the NASA NSIPP GCM, the Hadley Centre Atmospheric Model (HadAM3), the French IPSL LMDZ4, the GFDL AM2p10, and the GFDL AM2p12. The length of data for computing the SST climatology is 80 years for (g) the Hadley Centre model and (i) one of the GFDL models, and 100 years for all other models and the real world (1900–99).

TABLE 1. Atmospheric feedbacks (W m^{-2} K^{-1}) over the equatorial Pacific (5°S–5°N, 150°–250°E) from nine climate models. The net atmospheric feedback $[\partial(F_a)/\partial T] = [\partial(G_a)/\partial T] + [\partial(C_l)/\partial T] + [\partial(C_s)/\partial T] + [\partial(D_a)/\partial T]$. See text for the definition of the symbols for the various feedbacks. The values for these feedbacks are obtained through a linear regression using the interannual variations of the SST and the corresponding fluxes over the equatorial Pacific. The error bars are obtained using the method of Press et al. (1992) for the case in which the measurement errors of individual data points are not known. The numbers in parentheses are estimates from the ERA-40 reanalysis (the atmospheric transport Da is calculated as the difference between the net surface heat flux from the ERA-40 reanalysis and the net radiative flux at the top of the atmosphere from ERBE).

Process name	Observation	NCAR CAM1	NCAR CAM2	NCAR CAM3	NCAR CAM3 (T85)	NASA NSIPP-1	UKMO HadAM3	IPSL LMDZ4	GFDL AM2p10	GFDL AM2p12
					Feedback					
$\dfrac{\partial(G_a)}{\partial T}$	6.72 ± 0.27	9.10 ± 0.43	8.39 ± 0.41	8.89 ± 0.39	9.69 ± 0.36	8.21 ± 0.33	10.10 ± 0.48	8.95 ± 0.35	8.08 ± 0.33	9.43 ± 0.32
$\dfrac{\partial(C_L)}{\partial T}$	12.21 ± 1.03	15.94 ± 1.35	6.64 ± 0.63	7.21 ± 0.72	12.63 ± 0.82	9.14 ± 0.72	7.63 ± 0.86	14.85 ± 1.08	13.52 ± 0.78	14.74 ± 0.96
$\dfrac{\partial(G_a + C_l)}{\partial T}$	18.93 ± 1.17	25.03 ± 1.75	15.03 ± 0.96	16.11 ± 1.06	22.31 ± 1.05	17.34 ± 1.01	17.73 ± 1.31	23.80 ± 1.35	21.61 ± 1.05	24.17 ± 1.19
$\dfrac{\partial(C_s)}{\partial T}$	-10.93 ± 1.37	-4.98 ± 0.60	1.87 ± 0.96	-0.56 ± 0.78	-9.72 ± 1.09	-5.95 ± 0.77	-8.94 ± 1.33	-11.77 ± 1.40	-12.74 ± 0.79	-12.58 ± 1.09
$\dfrac{\partial(D_a)}{\partial T}$	-16.69 ± 1.51 (-18.73 ± 1.85)	-13.63 ± 1.76	-9.18 ± 1.40	-9.02 ± 1.20	-14.34 ± 1.23	-14.08 ± 0.96	-12.11 ± 1.53	-17.70 ± 1.08	-17.63 ± 0.92	-19.40 ± 1.28
$\dfrac{\partial(F_a)^*}{\partial T}$	-8.69 ± 1.76	6.42 ± 1.24	7.72 ± 1.12	6.53 ± 1.00	-1.75 ± 1.23	-2.69 ± 0.97	-3.33 ± 1.64	-5.67 ± 1.14	-8.77 ± 1.12	-7.81 ± 1.53
$\dfrac{\partial(F_s)}{\partial T}$	-14.89 ± 1.83 (-17.03 ± 2.06)	0.44 ± 1.24	1.48 ± 1.13	0.30 ± 1.02	-8.08 ± 1.25	-8.71 ± 0.98	-9.15 ± 1.64	-11.64 ± 1.14	-14.73 ± 1.13	-13.80 ± 1.53

and is termed the net atmospheric feedback and $\partial F_s/\partial T$ is the feedback from net surface heat flux into the ocean. Neglecting the heat storage in the atmosphere, which is small (Sun 2000), $\partial F_s/\partial T$ differs from $\partial F_a/\partial T$ by a constant—the rate of change of the ocean's surface emission with respect to SST. The numbers in parentheses are from the ERA-40 reanalysis. Feedbacks $\partial F_s/\partial T$ and $\partial D_a/\partial T$ estimated from the ERA-40 reanalysis are quite comparable to those from the NCEP–NCAR reanalysis.

With the exception of the two GFDL models and the French IPSL model, all models underestimate the negative feedback from the cloud albedo and the negative feedback from the atmospheric transport. The underestimate in the cloud albedo appears to be particularly worrisome, as this feedback in one of these models has the opposite sign to that observed. The NCAR CAM2 differs from the observed value in its simulation of the cloud albedo feedback by as much as 12.8 W m^{-2} K^{-1}. The NCAR CAM3 does not do much better. The NCAR CAM3 at T85 resolution, however, gets very close to the observed value. With the exception of the two GFDL models and the French model, the underestimates of the strength of the negative feedback from the atmospheric transport in these models are also significant. The error ranges from 2.4 W m^{-2} K^{-1} in the CAM3 at T85 resolution to 7.7 W m^{-2} K^{-1} in the NCAR CAM3 at the standard resolution.

All models have a stronger water vapor feedback than that indicated by ERBE observations. The differences between the modeled water vapor feedback and the feedback from the ERBE observations range from 15% to 50%. The GFDL AM2p10 has the smallest discrepancy with the ERBE observations in the simulation of the water vapor feedback, while the largest discrepancy is found in the Hadley Centre model. The differences between the water vapor feedback in the model simulations and that from ERBE observations could be, in part, due to the sampling differences between ERBE and the model data—the latter were obtained by the method in Cess and Potter (1988). Compared to the model data, ERBE undersamples the moist conditions (Zhang et al. 1994). Consequently, the ERBE observations may underestimate the changes of the greenhouse effect of water vapor from La Niña (cold and dry conditions) to El Niño (warm and moist conditions) and, therefore, underestimate the feedback of water vapor during ENSO. The bias due to the inadequate sampling does not explain the large range in the discrepancy between the water vapor feedback simulated by models and the water vapor feedback from ERBE observations. It may be prudent to continue to assume that, at least on a regional scale and during ENSO,

some models continue to have problems in simulating accurately the water vapor feedback. Note that the water vapor feedback referred to here includes the effect of water vapor as well as the lapse rate.

While it appears that some models may have significant errors in their simulations of water vapor feedback over the equatorial cold-tongue region, the results do not suggest that the corresponding feedbacks on a global scale also have significant errors. Indeed, since the work of Sun and Oort (1995) and Sun and Held (1996), there have been a number of studies looking at tropical or global mean changes in the greenhouse effect of water vapor (Soden 1997; Soden et al. 2002; Bauer et al. 2002; Allan et al. 2003). These studies generally conclude that the response of the tropical mean greenhouse effect of water vapor to El Niño warming is fairly close to that from observations. Further studies are needed to reconcile the differences seen on a regional scale with the agreements on a global scale. For now, it is noted that the tropical averaged signal of G_a associated with ENSO is much weaker than the signal right over the equatorial cold-tongue region because of cancellations between different regions (Fig. 2).

Models also vary on the estimate of the feedback from the longwave forcing of clouds, but they do not bias toward the same direction. While the NCAR CCM3 (CAM1) overestimates the feedback from the longwave forcing of clouds by 3.7 W m^{-2} K^{-1}, the NCAR CAM2 underestimates this feedback by 5.6 W m^{-2} K^{-1}. The underestimate of the feedback from the longwave forcing of clouds in the Hadley Centre model is also large (4.6 W m^{-2} K^{-1}). In four of the nine models—NCAR CAM2, NCAR CAM3, NASA/NSIPP, and HadAM3—there is a significant compensation between the error in the estimate of the feedback from the longwave forcing of clouds and the errors in the feedback from the greenhouse effect of water vapor; that is, the models that overestimate the water vapor feedback tend to underestimate the feedback from the longwave forcing of clouds. In these four models, the total feedback from the greenhouse effect of water vapor and clouds is much closer to its observed counterpart than either individual component. This again suggests that the model − observation differences could be in part due to the differences between the sampling method of ERBE and that of the model data.

The negative net atmospheric feedback in all models except the two GFDL models is underestimated over the region of concern. For most of these models, the underestimate of the strength of the net atmospheric feedback is because of the underestimate of the negative feedbacks from the cloud shortwave forcing and the atmospheric transport, and to a less degree because
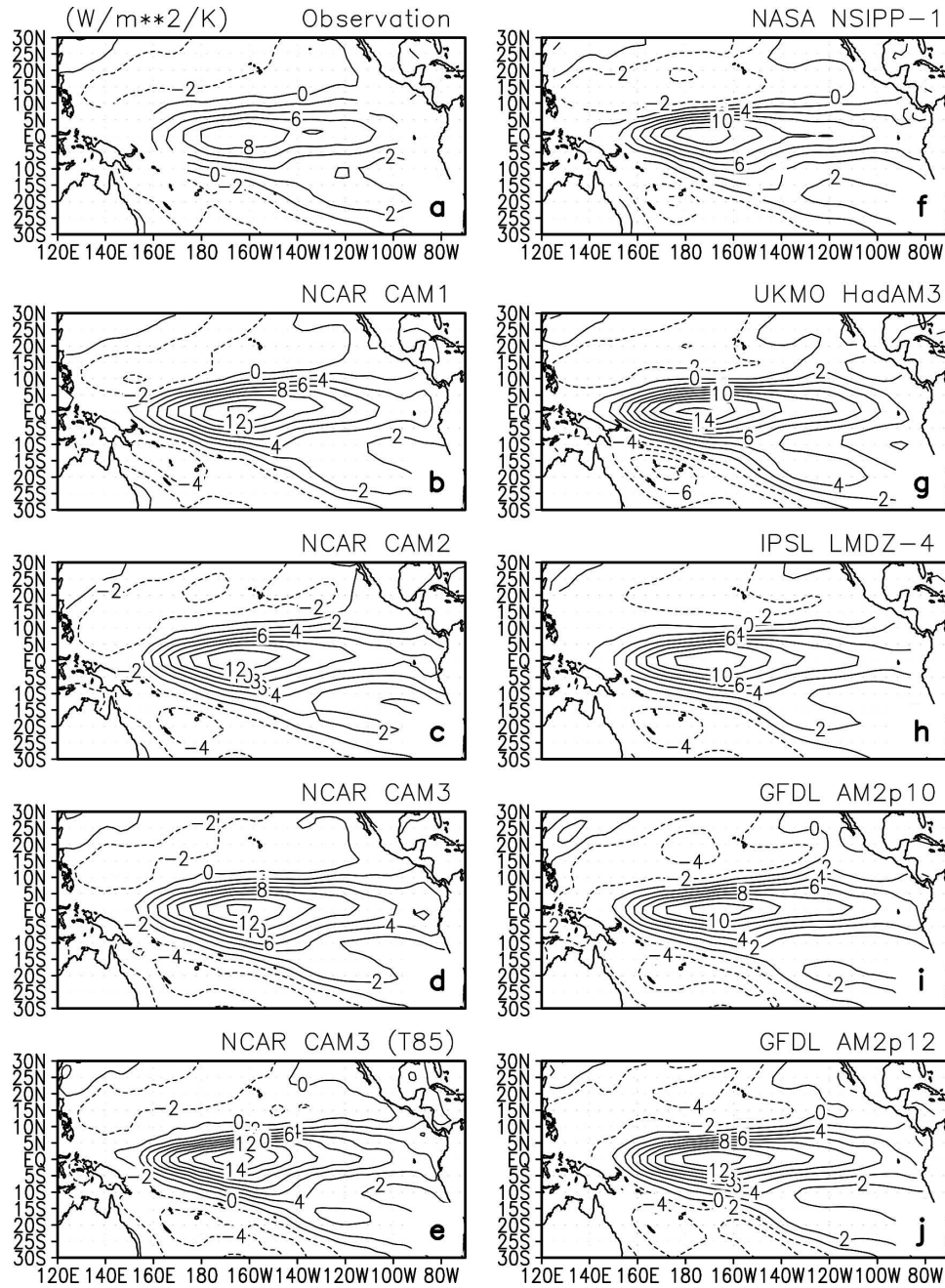
FIG. 2. Response of the greenhouse effect of water vapor (G_a) to El Niño warming. Shown are coefficients obtained by linearly regressing the greenhouse effect of water vapor at each grid point on the SST averaged over the equatorial Pacific (5°S–5°N, 150°–250°E). The interannual variations of G_a over the ERBE period are used for the calculations.

of the overestimate of the positive feedback from water vapor. For the French IPSL LMDZ4, an overestimate of the positive feedbacks from the greenhouse effect of water vapor and clouds is the dominant cause for the underestimate of the net negative feedback from the atmosphere and, hence, the regulating effect from the

atmosphere. The results confirm the suspicion that underestimating the regulatory effect from the atmosphere over the underlying SST in the region of concern is a prevalent problem in climate models. The results from the GFDL models (compared with other models), however, are very encouraging. The net atmospheric
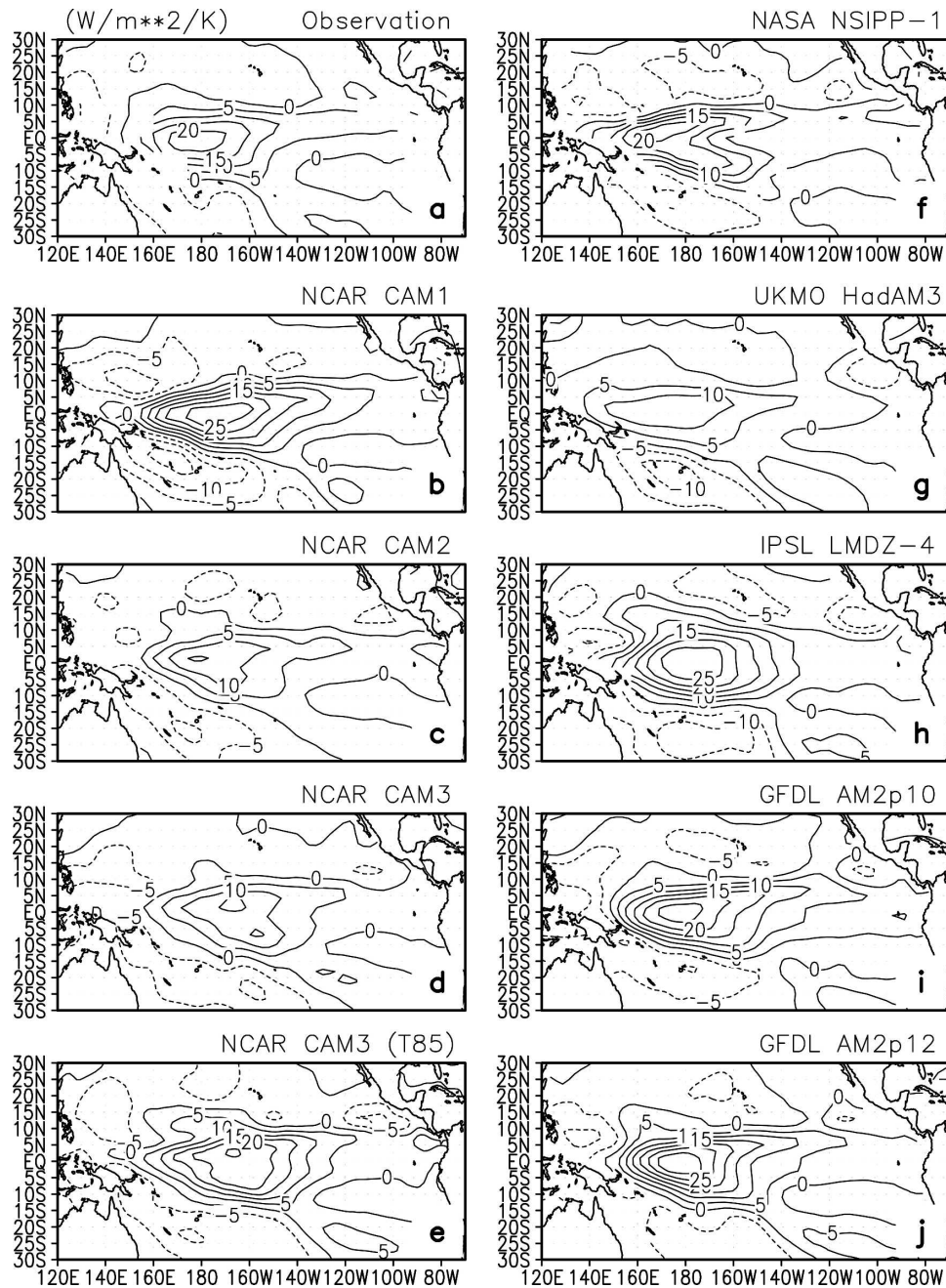
FIG. 3. Response of the greenhouse effect of clouds (C_l) to El Niño warming. Shown are coeffcents obtained by linearly regressing the greenhouse effect of clouds at each grid point on the SST averaged over the equatorial Pacific (5°S–5°N, 150°–250°E). The interannual variations of the concerned quantities over the ERBE period are used for the calculations.

feedback in the two GFDL models is comparable to the observed value. The improvements in the GFDL models (relative to CAM2/3) are not just from the improvements in the cloud albedo feedback, but also from the improvements in the feedback from the atmospheric transport.

The horizontal patterns of the response in G_a to ENSO forcing from the models show remarkable agreement with each other and with observations (Fig. 2). The corresponding response of C_l has more variability (Fig. 3). The NASA model is particularly notable: the response of C_l in the equatorial central Pacific near
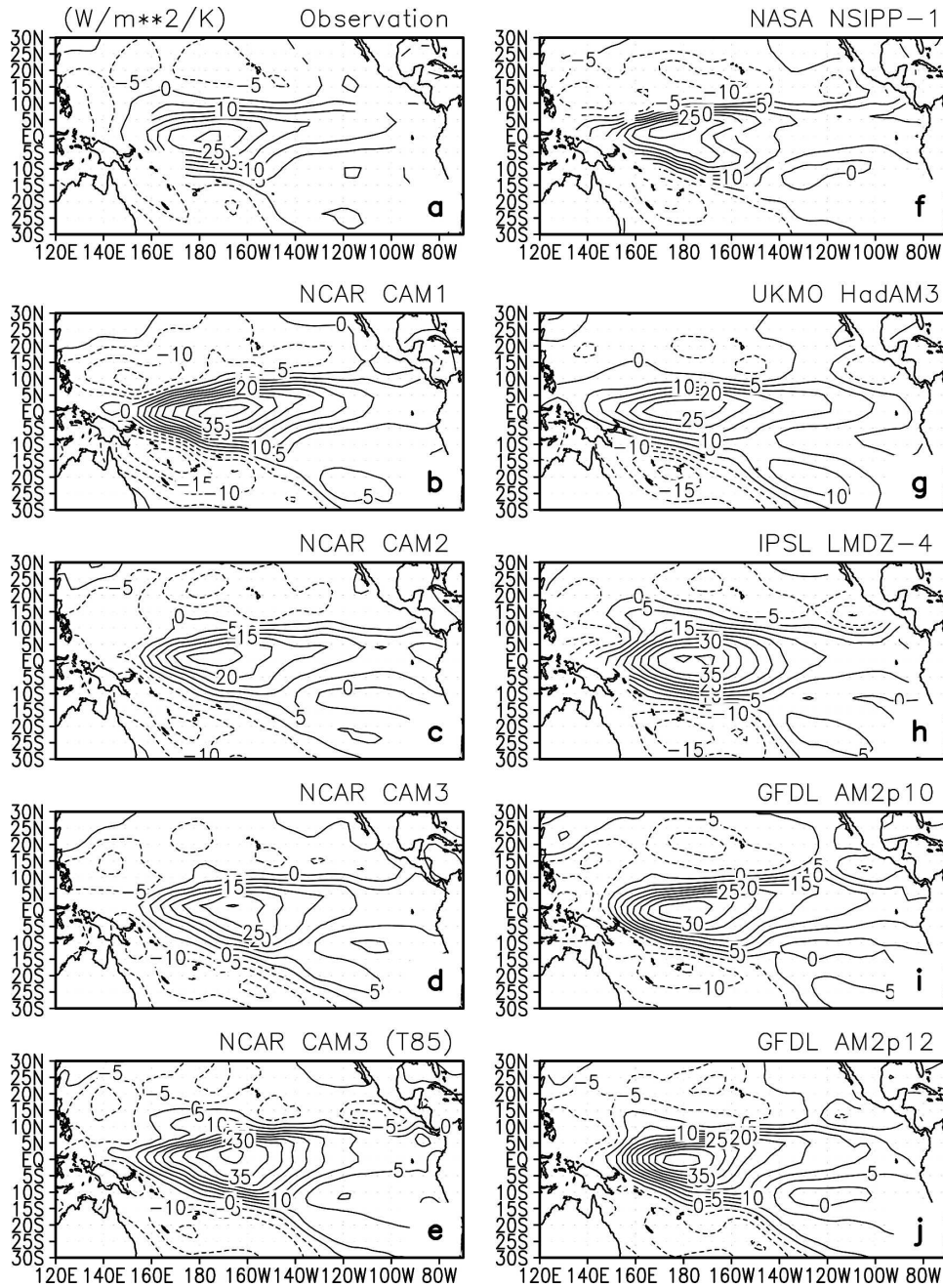
FIG. 4. As in Fig. 3, but for the combined greenhouse effect of clouds and water vapor ($G_a + C_l$).

the date line (180°–140°W) is much weaker than the observed (Fig. 3f). This equatorial minimum response splits the response of C_l to El Niño warming into two parts, each of which has a maximum off the equator. Such a split still exists when the response of G_a and the response of C_l are added together (Fig. 4f). It is again interesting to note, however, that the responses in the total greenhouse effect ($G_a + C_l$) in many of the models

have better agreement with that in the observations than the response of C_l alone (Fig. 4). Clearly, an overestimate of the total greenhouse effect is not a problem in all of the models.

The response of C_s and the rainfall in the NASA model also has the same "split pea" feature (cf. Fig. 5f with Fig. 6f), indicating a lack of response of convection in the central equatorial Pacific near the date line in the
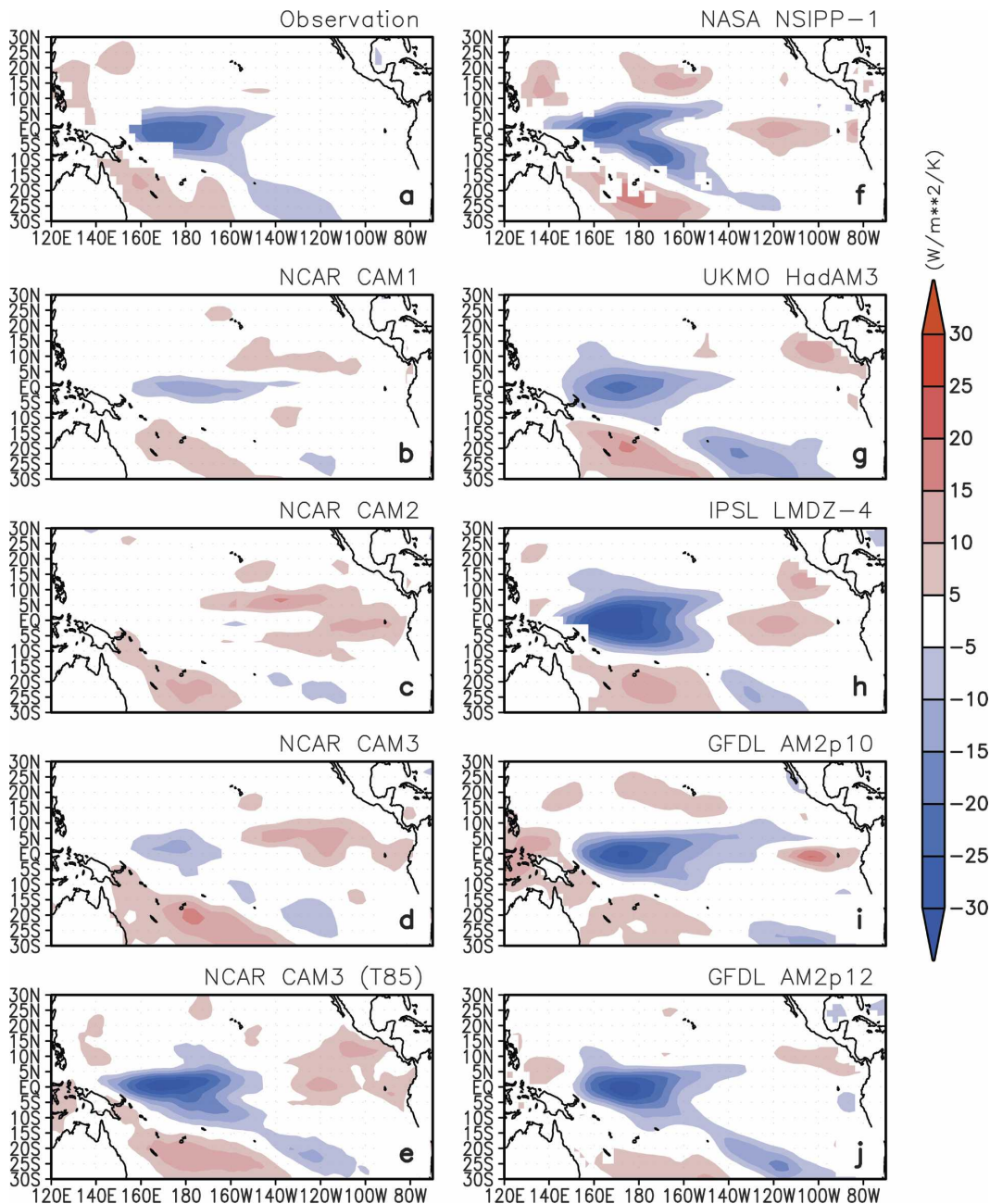
FIG. 5. As in Fig. 3, but for the shortwave forcing of clouds (C_s).

model. The lack of response of D_a in the same region in the NASA model (Fig. 7f) also suggests a lack of response of convection in the central equatorial Pacific.

Contrasting the spatial patterns in the response of the cloud forcing (Fig. 3 and Fig. 5) with the spatial patterns in the rainfall (Fig. 6) confirms the impression that the leading source of errors in the response of C_s may still be the most obvious: errors in the response of convection. The rainfall responses in the equatorial central

Pacific in CAM2 and CAM3 are the two weakest, so are their responses in C_s. The rainfall response in the CAM3 at T85 resolution is improved relative to the standard CAM3, so is the response of C_s. The improvements in the response in C_s in HadAM3 and the GFDL models (compared with CAM2 and CAM3) apparently also follow the improvement in the response of convection. All models predict a maximum precipitation response over the equator west of the date line, but the
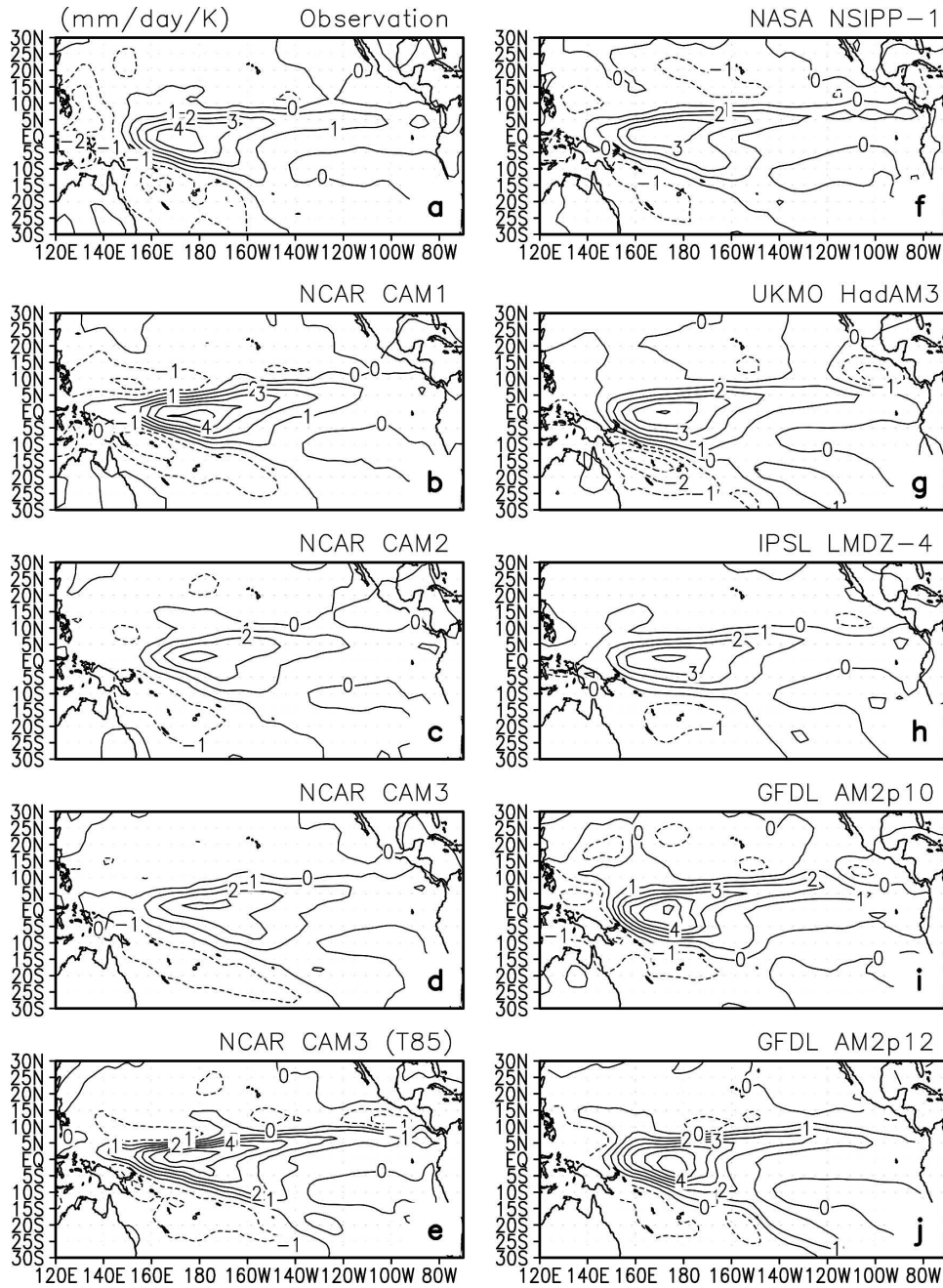
FIG. 6. As in Fig. 3, but for precipitation. Shown are coefficients obtained by linearly regressing the precipitation at each grid point on the SST averaged over the equatorial Pacific (5°S–5°N, 150°–250°E). The interannual variations of the concerned quantities over the ERBE period are used for the calculations. The observational data are from Xie and Arkin (1996).

GFDL models have the strongest responses in this region.

The response of convection in the model does not have the same control over the response of C_l as over the response of C_s: the HadAM3 has a response in rainfall that is slightly weaker than that in the observations, but the response in C_l in the same model is only about half of the value from the observations. Convection also has a lesser control over the response in G_a. For example, the rainfall in the NCAR CAM2 and
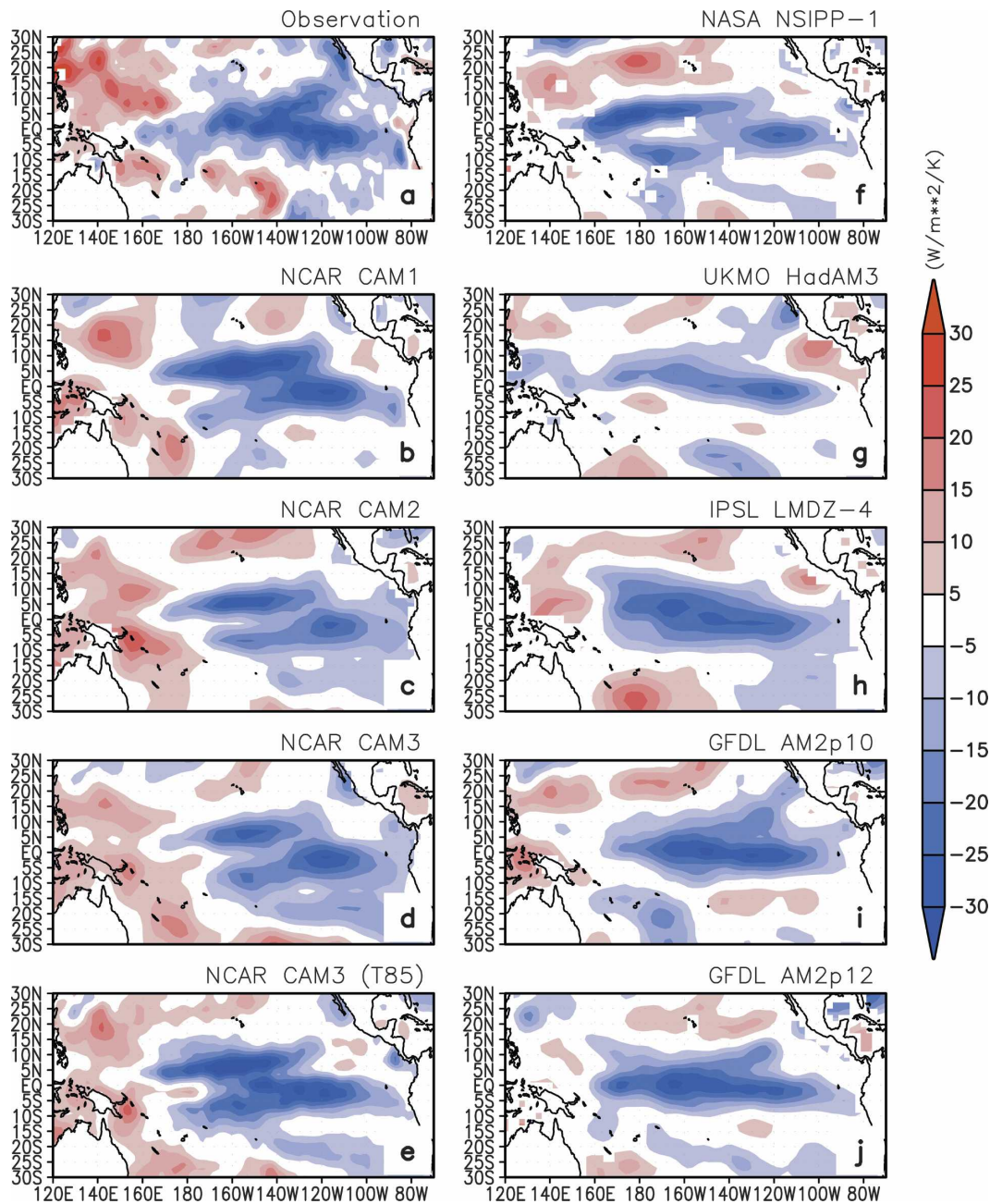
FIG. 7. As in Fig. 3, but for the convergence of vertically integrated transport of energy by the atmospheric circulations (D_a).

CAM3 is much weaker than that in CAM1, but the response in G_a in the NCAR CAM2 and CAM3 models is only slightly weaker than that in CAM1.

The two GFDL models and the French model simulate reasonably well the spatial pattern of the response in D_a; all other models do not (Fig. 7). The spatial patterns of the response in D_a in the four NCAR models are similar to each other—they all have a much weaker negative response over the equatorial central

Pacific (180°–140°W). Over this region, the maximum response of D_a in these models is located off the equator. The NASA model exhibits a similar feature.

The impact of the errors in the aforementioned feedbacks on the response of the net surface heating (F_s) is further shown in Fig. 8, which gives a basinwide, and more critical, view of the response of the model atmosphere. In five of the nine models (the NCAR CAM1, CAM2, CAM3 at T42 resolution, CAM3 at T85 reso-
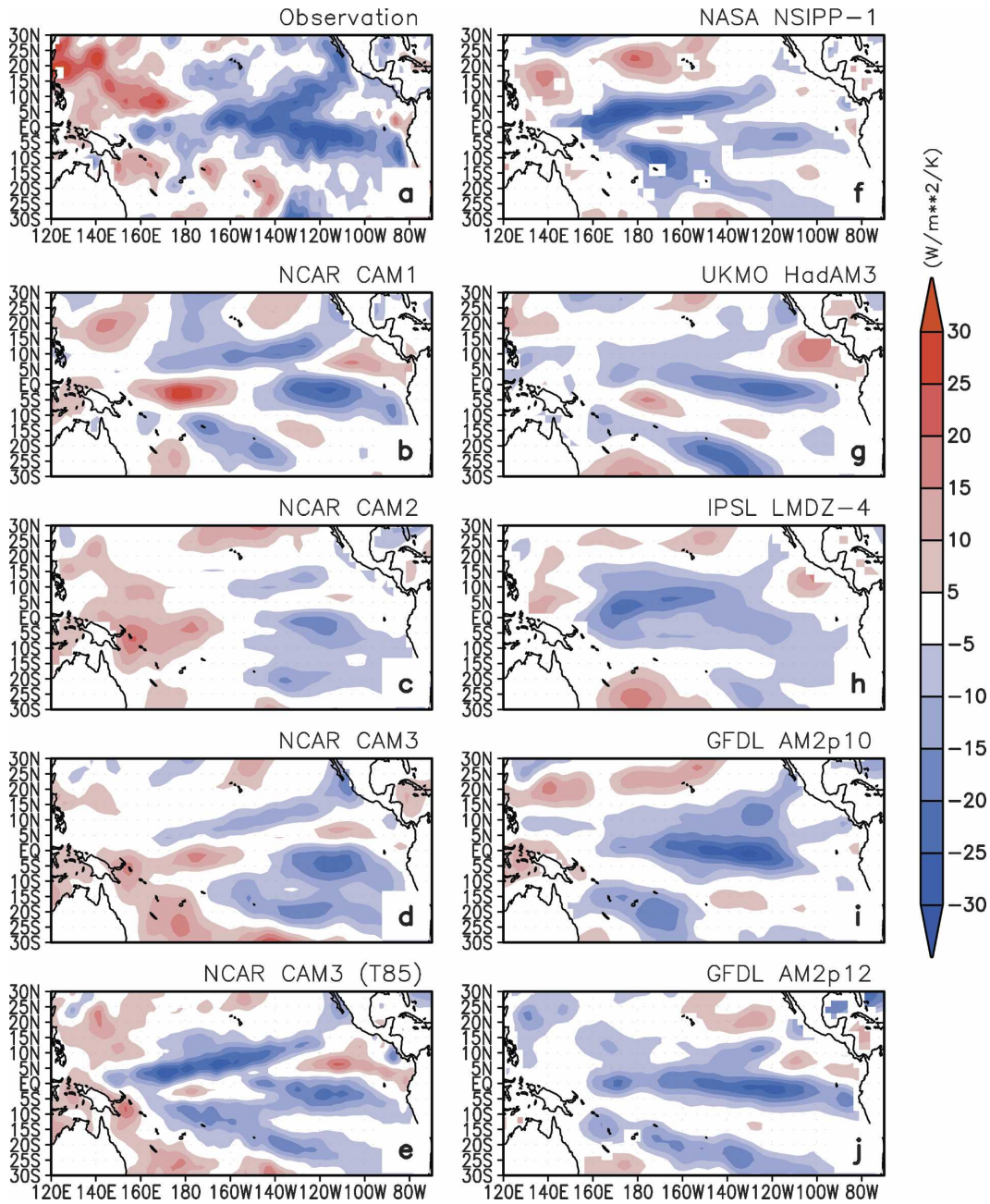
FIG. 8. As in Fig. 3, but for the net surface heating (F_s). The observational data used for F_s are the same as in Sun et al. (2003).

lution, and the NASA model), the response of the surface heating to El Niño warming in the equatorial central Pacific (160°E–140°W) has the wrong sign. The response of F_s in the Hadley Centre model in the same region is near zero. The response of F_s in the French model has the correct sign in the region of concern, but weaker magnitude. The two GFDL models have adequate responses in the equatorial central Pacific. One of them—the GFDL AM2p10—suffers a significant de-

ficiency in the region east to about 120°W. The negative response in the GFDL AM2p10 also does not extend as far west as in the observations. The zonal extent of the response in the later version of the GFDL model—the AM2p12—is improved, but the meridional extent of the response is more confined. Nonetheless, the spatial pattern of the response of F_s in both the GFDL models resembles the observed remarkably well.

Diagnosing the root causes of all the model deficien-

cies is beyond the scope of the present paper and would require more sophisticated tools than the simple regression analysis here. The encouraging part of the present analysis is that it is possible for the model atmosphere to have a regulating effect comparable in strength to the real atmosphere: the GFDL AM2p10 provides an example. Whether this good agreement between the simulations by the GFDL model and the observations is simply a matter of luck or truly reflects the fidelity of the model to nature needs to be further examined. For now, we note that the precipitation response over the equator in the GFDL models is stronger than in the observations. In fact, normalizing the maximum precipitation response over the equator, the two GFDL models still underestimate the strength of the negative feedback from cloud albedo. The feedback from the total greenhouse effect in the GFDL AM2p12 also appears to be too strong to be explained by the possible errors in the ERBE observations.

4. Discussion

These results confirm the suspicion that an underestimate of the regulatory effect from the atmosphere over the equatorial Pacific region is a prevalent problem. Most models underestimate the strength of the negative feedback from cloud albedo and the strength of the negative feedback from atmospheric transport. The underestimate of the strength of these negative feedbacks is linked to an underestimate of the response of precipitation over the equator. All models have a stronger water vapor feedback than that indicated in ERBE observations. The degree of the overestimate of the water vapor feedback varies considerably among the models.

While the analysis has revealed some common deficiencies in the simulation of atmospheric feedbacks by GCMs, the results also suggest that the common errors in the atmospheric feedbacks are unlikely the sole cause of the excessive cold tongue in the central equatorial Pacific. The simulation of the strength of the net atmospheric feedback in the GFDL AM2p10 is probably as close to the observed as one can reasonably hope, but the corresponding coupled model still has an excessive cold tongue (Fig. 1i). The results highlight the need to look at the ocean feedbacks. One way to do so is to check the response of the surface wind stress to changes in the SST and then the response of the ocean heat transport to the changes in the wind stress. The former can be assessed to some degree using the AMIP runs of the atmospheric GCMs. The obstacle in carrying out this analysis immediately is the lack of good data for the tropical wind stress. The limited satellite

data (Liu 2002) has revealed severe deficiencies in the NCEP–NCAR reanalysis, but the satellite dataset is still too short for calculating feedbacks. The latter requires forced ocean experiments from different groups using the same surface forcing. These forced ocean model experiments are not yet available on the scale of the AMIP experiments. Nor is it clear whether the accuracy of ocean heat transport data is sufficient to validate the results from the model experiments.

The present analysis has a linear perspective built in, and therefore the results are more relevant for the initial development of the excessive cold tongue. After a significant cold SST bias in the central equatorial Pacific develops in the modeled climate, it may displace the convection so far west that the associated atmospheric feedbacks cease operating in the central equatorial Pacific. The study by Wittenberg et al. (2004) suggests that GFDL models may have this nonlinear effect. Other models probably have this nonlinear effect too. Nonetheless, it is logical to first identify the factors that are responsible for the initial growth of the excessive cold tongue and then examine how the excessive cold tongue in the coupled model maintains its stability. This consideration of priorities points us in a direction to extend the present study, which is to directly use the outputs from coupled models to quantify the feedbacks in the cold-tongue region. The drawback of using the ENSO signals in the coupled models is that the signals are not the same as in the real world, but the results may shed light on the question of how the excessive cold tongue in the coupled model maintains its stability.

Underestimating the negative feedbacks in the central equatorial Pacific does not suggest that the models overestimate global warming. What has been assessed here are regional feedbacks on the time scale of ENSO. The forcing due to increases in CO_2 is not the same as the El Niño warming. While bearing this difference in mind, one also notes that many coupled GCMs do predict El Niño–like warming in response to increases in CO_2 (Meehl and Washington 1996; Timmerman et al. 1999; Cai and Whetton 2000; Boer et al. 2004). Therefore, the feedbacks inferred from the response to El Niño warming may not be entirely irrelevant to the feedbacks in global warming. In any case, our confidence in the model predictions of global warming may have to come from how well the models simulate the feedbacks on shorter time scales because it is over these time scales that we have better data and know more quantitatively the feedbacks in nature.

REFERENCES

Allan, R. P., M. A. Ringer, and A. Slingo, 2003: Evaluation of moisture in the Hadley Centre climate model using simulations of HIRS water-vapor channel radiances. *Quart. J. Roy. Meteor. Soc.,* **129,** 3371–3389.

Barkstrom, B. R., E. F. Harrison, G. L. Smith, R. Green, J. Kibler, and R. D. Cess, and the ERBE Science Team, 1989: Earth Radiation Budget Experiment (ERBE) archive and April 1985 results. *Bull. Amer. Meteor. Soc.,* **70,** 1254–1262.

Bauer, M., A. D. Del Gienio, and J. R. Lanzante, 2002: Observed and simulated temperature–humidity relationships: Sensitivity to sampling and analysis. *J. Climate,* **15,** 203–215.

Boer, G. J., B. Yu, S.-J. Kim, and G. M. Flato, 2004: Is there observational support for an El Niño-like pattern of future global warming? *Geophys. Res. Lett.,* **31,** L06201, doi:10.1029/2003GL018722.

Boville, B. A., and P. R. Gent, 1998: The NCAR Climate System Model, version one. *J. Climate,* **11,** 1115–1130.

Cai, W., and P. H. Whetton, 2000: Evidence for a time-varying pattern of greenhouse warming in the Pacific Ocean. *Geophys. Res. Lett.,* **27,** 2577–2580.

Cess, R. D., and G. L. Potter, 1988: A methodology for understanding and intercomparing atmospheric climate feedback processes in general circulation models. *J. Geophys. Res.,* **93,** 8305–8314.

Chou, M.-D., and M. J. Suarez, 1996: A solar radiation parameterization (CLIRAD-SW). NASA Tech. Memo. 104606, Vol. 15, 48 pp.

Collins, M., S. F. B. Tett, and C. Cooper, 2001: The internal climate variability of a HadCM3, a version of the Hadley Centre coupled model without flux adjustments. *Climate Dyn.,* **17,** 61–81.

Collins, W. D., and Coauthors, 2003: Description of the NCAR Community Atmosphere Model (CAM2). 189 pp. [Available online at http://www.ccsm.ucar.edu/models/atm-cam/docs/cam2.0/description.pdf.]

——, and Coauthors, 2004: Description of the NCAR Community Atmosphere Model (CAM 3.0). NCAR Tech. Rep. NCAR/TN-464+STR, Boulder, CO, 210 pp.

Delworth, T. L., and Coauthors, 2006: GFDL's CM2 global coupled climate models. Part I: Formulation and simulation characteristics. *J. Climate,* **19,** 643–674.

Emanuel, K. A., 1991: A scheme for representing cumulus convection in large-scale models. *J. Atmos. Sci.,* **48,** 2313–2335.

Fu, R., A. D. DelGenio, W. B. Rossow, and W. T. Liu, 1990: Cirrus cloud thermostat for tropical sea surface temperature tested using satellite data. *Nature,* **358,** 394–397.

GFDL Global Atmospheric Model Development Team, 2004: The new GFDL global atmosphere and land model AM2/LM2: Evaluation with prescribed SST simulations. *J. Climate,* **17,** 4641–4673.

Grandpeix, J.-Y., V. Phillips, and R. Tailleux, 2004: Improved mixing representation in Emanuel's convection scheme. *Quart. J. Roy. Meteor. Soc.,* **130,** 3207–3222.

Gregory, D., and P. R. Rowntree, 1990: A mass flux convection scheme with representation of cloud ensemble characteristics and stability-dependent closure. *Mon. Wea. Rev.,* **118,** 1483–1506.

Hack, J. J., 1994: Parameterization of moist convection in the National Center for Atmospheric Research Community Climate Model (CCM2). *J. Geophys. Res.,* **99,** 5551–5568.

Kiehl, J. T., 1998: Simulation of the tropical Pacific warm pool with the NCAR Climate System Model. *J. Climate,* **11,** 1342–1355.

——, and P. R. Gent, 2004: The Community Climate System Model, version 2. *J. Climate,* **17,** 3666–3682.

——, J. J. Hack, G. Bonan, B. A. Boville, D. Williamson, and P. J. Rasch, 1998: The National Center for Atmospheric Research Community Climate Model: CCM3. *J. Climate,* **11,** 1131–1149.

Liu, W. T., 2002: Progress in scatterometer applications. *J. Oceanogr.,* **58,** 121–136.

Lock, A. P., A. R. Brown, M. R. Bush, G. M. Martin, and R. N. B. Smith, 2000: A new boundary layer mixing scheme. Part I: Scheme description and single-column model tests. *Mon. Wea. Rev.,* **128,** 3187–3199.

Marti, O., and Coauthors, cited 2005: The new IPSL climate system model: IPSL CM4. [Available online at http://dods.ipsl.jussieu.fr/omamce/IPSLCM4/DocIPSLCM4/FILES/DocIPSLCM4.pdf.]

Meehl, G. A., and W. M. Washington, 1996: El Niño-like climate change in a model with increased atmospheric CO_2 concentrations. *Nature,* **382,** 56–60.

Mellor, G. L., and T. Yamada, 1974: A hierarchy of turbulence closure models for planetary boundary layers. *J. Atmos. Sci.,* **31,** 1791–1806.

Moorthi, S., and M. Suarez, 1992: Relaxed Arakawa–Schubert: A parameterization of moist convection for general circulation models. *Mon. Wea. Rev.,* **120,** 978–1002.

Murtugudde, R., J. Beauchamp, C. R. McClain, and A. J. Busalacchi, 2002: Effects of penetrative radiation on the upper tropical ocean circulation. *J. Climate,* **15,** 470–496.

Pierrehumbert, R. T., 1995: Thermostats, radiator fins, and the local runaway greenhouse. *J. Atmos. Sci.,* **52,** 1784–1806.

Press, W. H., S. A. Teukolsky, W. T. Vetterling, and B. P. Flannery, 1992: *Numerical Recipes.* Cambridge University Press, 963 pp.

Ramanathan, V., and W. Collins, 1991: Thermodynamic regula-

tion of ocean warming by cirrus clouds deduced from observations of the 1987 El Niño. *Nature,* **351,** 27–32.

Rayner, N. A., E. B. Horton, D. E. Parker, C. K. Folland, and R. B. Hackett, 1996: Version 2.2 of the Global Sea-Ice and Sea Surface Temperature Data Set, 1903–1994. Climate Research Tech. Note 74 (CRTN74), Hadley Centre for Climate Prediction and Research, Met Office, Exeter, Devon, United Kingdom, 35 pp.

Soden, B. J., 1997: Variations in the tropical greenhouse effect during El Niño. *J. Climate,* **10,** 1050–1054.

——, R. T. Wetherald, G. L. Stenchikov, and A. Robock, 2002: Global cooling after the eruption of Mount Pinatubo: A test of climate feedback by water vapor. *Science,* **296,** 727–730.

——, A. J. Broccoli, and R. S. Hemler, 2004: On the use of cloud forcing to estimate cloud feedbacks. *J. Climate,* **17,** 3661–3665.

Stockdale, T. N., A. J. Busalacchi, D. E. Harrison, and R. Seager, 1998: Ocean modeling for ENSO. *J. Geophys. Res.,* **103,** 14 325–14 355.

Suarez, M. J., 1995: Documentation of the ARIES/GEOS Dynamical Core, version 2. NASA Tech. Memo. 104606, Vol. 5, 53 pp

Sun, D.-Z., 2000: The heat sinks and sources of the 1986–87 El Niño. *J. Climate,* **13,** 3533–3550.

——, and A. H. Oort, 1995: Humidity–temperature relationships in the tropical troposphere. *J. Climate,* **8,** 1974–1987.

——, and I. Held, 1996: A comparison of modeled and observed relationships between interannual variations of water vapor and temperature. *J. Climate,* **9,** 665–675.

——, and Z. Liu, 1996: Dynamic ocean–atmosphere coupling: A thermostat for the tropics. *Science,* **272,** 1148–1150.

——, and K. E. Trenberth, 1998: Coordinated heat removal from the tropical Pacific region during the 1986–87 El Niño. *Geophys. Res. Lett.,* **25,** 2659–2662.

——, J. Fasullo, T. Zhang, and A. Roubicek, 2003: On the radiative and dynamical feedbacks over the equatorial Pacific cold tongue. *J. Climate,* **16,** 2425–2432.

Timmerman, A. J., J. Oberhuber, A. Bacher, M. Esch, M. Latif, and E. Roeckner, 1999: Increased El Niño frequency in a climate model forced by future global warming. *Nature,* **398,** 694–696.

Trenberth, K. E., and C. J. Guillemot, 1998: Evaluation of the atmospheric moisture and hydrological cycle in the NCEP reanalyses. *Climate Dyn.,* **14,** 213–231.

——, J. M. Caron, and D. P. Stepaniak, 2001: The atmospheric energy budget and implications for surface fluxes and ocean heat transport. *Climate Dyn.,* **17,** 259–296.

Uppala, S., and Coauthors, 2004: ERA-40: ECMWF 45 year reanalysis of the global atmosphere and surface conditions 1957–2002. *ECMWF Newsletter*, No. 101, ECMWF, Reading, United Kingdom, 2–21.

Wallace, J. M., 1992: Effect of deep convection on the regulation of tropical sea surface temperature. *Nature,* **357,** 230–231.

Wetherald, R. T., and S. Manabe, 1988: Cloud feedback processes in a general circulation model. *J. Atmos. Sci.,* **45,** 1397–1415.

Wittenberg, A. T., A. Rosati, N.-C. Lau, and J. J. Ploshay, 2004: GFDL's CM2 global coupled models. Part III: Tropical Pacific climate and ENSO. *J. Climate,* **19,** 698–722.

Xie, P., and P. A. Arkin, 1996: Analyses of global monthly precipitation using gauge observations, satellite estimates, and numerical model predictions. *J. Climate,* **9,** 840–858.

Yanai, M., S. Esbensen, and J.-H. Chu, 1973: Determination of bulk properties of tropical cloud clusters from large-scale heat and moisture budgets. *J. Atmos. Sci.,* **30,** 611–627.

Zhang, G. J., and N. A. McFarlane, 1995: Sensitivity of climate simulations to the parameterization of cumulus convection in the Canadian Climate Centre general circulation model. *Atmos.–Ocean,* **33,** 407–446.

Zhang, M. H., R. D. Cess, T. Y. Kwon, and M. H. Chen, 1994: Approaches of comparison for clear-sky radiative fluxes from general circulation models with Earth Radiation Budget Experiment data. *J. Geophys. Res.,* **99,** 5515–5523.